

2011

Length scales of interactions in magnetic, dielectric, and mechanical nanocomposites

Ralph Skomski

University of Nebraska-Lincoln, rskomski2@unl.edu

Balamurugan Balamurugan

University of Nebraska-Lincoln, balamurugan@unl.edu

Eva Schubert

University of Nebraska-Lincoln, efranke3@unl.edu

Axel Enders

University of Nebraska-Lincoln, a.enders@me.com

David J. Sellmyer

University of Nebraska-Lincoln, dsellmyer@unl.edu

Follow this and additional works at: <http://digitalcommons.unl.edu/physicsenders>



Part of the [Physics Commons](#)

Skomski, Ralph; Balamurugan, Balamurugan; Schubert, Eva; Enders, Axel; and Sellmyer, David J., "Length scales of interactions in magnetic, dielectric, and mechanical nanocomposites" (2011). *Axel Enders Publications*. 36.
<http://digitalcommons.unl.edu/physicsenders/36>

This Article is brought to you for free and open access by the Research Papers in Physics and Astronomy at DigitalCommons@University of Nebraska - Lincoln. It has been accepted for inclusion in Axel Enders Publications by an authorized administrator of DigitalCommons@University of Nebraska - Lincoln.

Length scales of interactions in magnetic, dielectric, and mechanical nanocomposites

R. Skomski, B. Balamurugan, E. Schubert,* A. Enders, and D. J. Sellmyer

*Department of Physics and Astronomy and Center for Materials Research and Analysis,
University of Nebraska, Lincoln, NE 68588*

**Department of Electrical Engineering, University of Nebraska, Lincoln, Nebraska*

ABSTRACT

It is investigated how figures of merits of nanocomposites are affected by structural and interaction length scales. Aside from macroscopic effects without characteristic lengths scales and atomic-scale quantum-mechanical interactions there are nanoscale interactions that reflect a competition between different energy contributions. We consider three systems, namely dielectric media, carbon-black reinforced rubbers and magnetic composites. In all cases, it is relatively easy to determine effective materials constants, which do not involve specific length scales. Nucleation and breakdown phenomena tend to occur on a nanoscale and yield a logarithmic dependence of figures of merit on the macroscopic system size. Essential system-specific differences arise because figures of merits are generally nonlinear energy integrals. Furthermore, different physical interactions yield different length scales. For example, the interaction in magnetic hard-soft composites reflects the competition between relativistic anisotropy and nonrelativistic exchange interactions, but such hierarchies of interactions are more difficult to establish in mechanical polymer composites and dielectrics.

Keywords: Maxwell-Garnett equation, Bruggeman composites; Dielectric Energy Density; Breakdown; Fracture; Polymers; Rubber; Nanocomposites; Coercivity; Energy Product

INTRODUCTION

Nanocomposites are widely used in technology, because they combine the advantages of single-phase materials and range from naturally occurring biological structures and traditional materials to artificial materials used in transport, space, microelectronic, and other high-tech applications. Examples are naturally occurring skeletal materials, such as bones and wood, whose nanostructure ensures stiffness without brittleness, and in artificial mechanical materials, such as concrete, fiber composites, reinforced polymers for car tires to [1, 2, 3]. In magnetism, aligned two-phase permanent magnets have been predicted to yield energy products beyond those of single-phase rare-earth permanent magnets [4]. Many multiferroic and multifunctional materials are also structured as two-phase composites. Some of these structures are straightforward mixtures, but many exhibit macroscopic or nanoscale interactions between the phases.

Examples are magnet-polymer composites, which have been investigated in the light of future applications such as materials with negative index of refraction [5, 6, 7].

A traditional approach to composite materials is the description in terms of effective materials constants. Some mixtures of materials obey mixing rules of the type

$$A_{\text{eff}} = (1 - f) A_m + f A_i \quad (1)$$

where A_i and A_m are the materials constants of the matrix and inclusion phases, respectively, and f is the volume fraction of the inclusion phase. However, Eq. (1) is limited to noninteracting mixtures and to interacting phases where $A_i \approx A_m$. Consider, for example, the resistivity of insulating oxide particles ($\rho_i = \infty$) in a metallic matrix of finite resistivity ρ_m . For arbitrarily small but nonzero volume fractions f , Eq. (1) then leads to the unphysical prediction of an infinite resistivity $\rho_{\text{eff}} = \infty$ ($A_{\text{eff}} = \infty$). Similar violations of the mixing rule exist in other systems. For instance, dielectric and magnetic susceptibilities rarely obey Eq. (1).

For small volume fractions, the unphysical divergences are removed by using the generalized Maxwell-Garnett equation

$$A_{\text{eff}} = A_m \left(1 + f \frac{A_i - A_m}{g A_i + (1 - g) A_m} \right) \quad (2)$$

This equation contains a shape parameter g , which can be derived for specific systems by explicit single-inclusion calculations. Examples are dielectrics [8], magnets [9, 10], conductors [10], and mechanical composites [2, 11, 12]. In many but not all cases (see below), the shape factor is equal to the inclusion's depolarizing factor, $g = N$. In particular, $N = 1/3$ for spheres, $N = 0$ for strongly elongated ellipsoids (rods or needles) and $N = 1$ for oblate or flat ellipsoids (platelets). Figure 1 shows the geometry of typical composites. Most of these structures can be prepared by traditional methods, but some need new approaches, such as glancing-angle deposition (GLAD) onto rotating substrates in the case of magnetic nanospirals [13]. The extension to arbitrary volume fractions is generally nontrivial, but there exists a powerful effective-medium approach known as the *Bruggeman theory* [1], which covers arbitrary volume fractions and percolation phenomena on a mean-field level (see next section).

The question arises how nanoscale interactions affect the performance of composite materials and whether the underlying physics exhibits universal tendencies across systems and phenomena. This question has three important ramifications. First, figures of merit such as the electrostatic energy density stored in dielectrics, the energy product of permanent magnets and the energy dissipated in viscoelastic composites, are integrals over nonlinear functions, and different figures of merit may be differently affected by nanoscale inhomogeneities. Second, effective materials constants are only one aspect of the performance of composites. Phenomena such as dielectric breakdown, coercivity, and mechanical fracture usually involve nanoscale materials imperfections and are poorly described by effective medium theories [4, 9, 14]. Third, nanoscale interactions directly modify the materials constants when the structural features size becomes comparable to the nanoscale interaction lengths. The purpose of this paper is to analyze how these mechanisms operate in nanostructures, comparing various systems and elaborating similarities and differences.

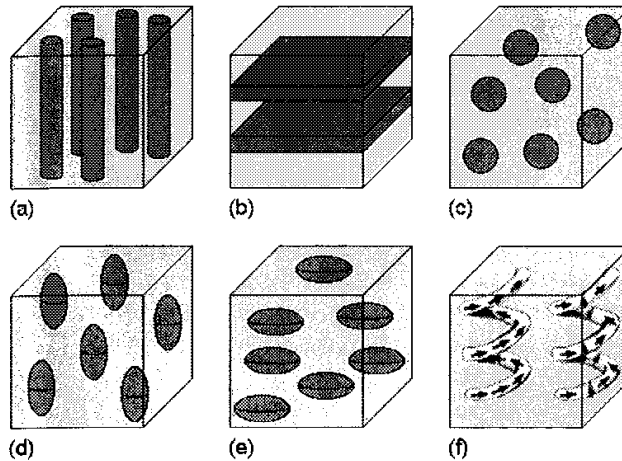


Fig. 1. Geometry and depolarization factors for some two-phase nanostructures: (a) rods ($N = 0$), (b) platelets ($N = 1$), (c) spheres ($N = 1/3$), (d) prolate ellipsoids ($N < 1/3$), (e) oblate ellipsoids ($N > 1/3$), and (f) nanospirals.

SCIENTIFIC BACKGROUND: BRUGGEMAN MODEL

The Bruggeman approach is a length-scale-free and selfconsistent mean-field method to calculate materials properties of composites [1, 15]. The idea is to start from the Maxwell-Garnett equation (1) and to treat arbitrary volume fractions f by selfconsistently embedding the matrix and inclusion phases in an effective medium. It is also known as the Polder–van Santen formula, self-consistent field theory (SCF) or simply effective medium theory [16, 17]. In solid state physics, the Bruggeman theory is closely related to the coherent-potential approximation (CPA) for binary alloys [18, 19, 20].

The theory was originally derived for dielectric materials but can be used for a broad variety of static and dynamic phenomena. Examples are effective dielectric susceptibilities (static and dynamic dielectric response of inhomogeneous media, materials with negative index of refraction) [10, 21], effective magnetic permeability [4, 10, 22, 23], optical properties [8, 21], mechanical composites (elasticity of reinforced construction materials and filled polymers, such as car tires) [12, 20, 23, 24], geoscience [17], rheology (viscosity and viscoelasticity of colloidal suspensions, such as blood, food, gels) [25], electrical conduction (insulating inclusions in metals and metal-superconductor composites) [10, 26, 27], thermal conduction (heat insulation using composite construction materials) [10], and diffusivity (hydrogen transport) [10]. In general, both isotropic and anisotropic composites can be treated [26, 23, 28, 29].

The starting point is a generalized potential $\Phi(\mathbf{r})$ whose negative gradient is the (generalized) field, $\mathbf{f} = -\nabla\Phi$. For example, the electric field in a static dielectric can be written as $\mathbf{E} = -\nabla\Phi$. The field creates a generalized flux density \mathbf{b} , and this flux density is described by the materials equation $\mathbf{b} = A \mathbf{f}$, where A is a generalized materials constant (compliance). In the dielectric analogy, this is the electric permeability. The flux is

usually fed into the system by applying an external force or field but has no sources inside the material, so that $\nabla \mathbf{b} = 0$. This yields the flux-conservation relation

$$\nabla \cdot (A(\mathbf{r}) \nabla \Phi) = 0 \quad (3)$$

In any single-phase region of the composite, this reduces to $\nabla^2 \Phi = 0$, accompanied by appropriate boundary conditions. This equation does not contain any characteristic length, so that it can be used for macroscopic, micron-size and nanoscale inclusions. The respective parallel and perpendicular components of the force \mathbf{f} and of the flux density \mathbf{b} , are continuous at interfaces, and far away from the inclusion, the field $\mathbf{f} = -\nabla \Phi(\mathbf{r})$ is homogeneous. The solution of Eq. (3) yields the Maxwell-Garnett equation [2, 10, 12, 15, 23, 24].

In contrast to Eq. (2), which is limited to small volume fractions f , the Bruggeman approach describes arbitrary f on a mean-field level. This is achieved by selfconsistently embedding both phases in an effective medium averaging over the total volume. The procedure yields

$$f \frac{A_i - A_{\text{eff}}}{g A_i + (1 - g) A_{\text{eff}}} + (1 - f) \frac{A_m - A_{\text{eff}}}{g A_m + (1 - g) A_{\text{eff}}} = 0 \quad (4)$$

which is basically a quadratic equation for A_{eff} . Aside from the input parameters A_m , A_i , and f , Eq. (3) contains a single parameter, namely the shape constant g . This parameter depends on the considered physical property and on the geometry of the composites. Many electromagnetic and transport systems belong to the first group, where $g = N$. In particular, $g = 0$ for long needles, $g = 1/3$ for spherical inclusions, and $g = 1$ for multilayers of embedded plates [23, 30]. In mechanical composites, $g \neq N$ depends on Poisson's ratio and on the considered elastic modulus, because Eq. (3) must be modified [2, 23].

Equation (4) yields a *percolation* transition with a dimensionality-independent mean-field exponent $\gamma = 1$ [19]. For example, metallic regions in an insulator do not affect the resistivity until the metallic volume fraction reaches the percolation threshold $f_c = 1/3$. By putting $A_i = 0$ and investigating the transition $A_{\text{eff}} \rightarrow 0$ we obtain a threshold $f_c = 1 - g$, whereas $A_i = \infty$ and $A_{\text{eff}} \rightarrow \infty$ yields $f = g$. The metal-insulator percolation threshold $f_c = g$ is obtained by considering the effect of insulating inclusions ($\sigma = \infty$) in a metallic matrix ($\sigma = \sigma_m$), which yield volume fractions of $1 - g = 2/3$ for the insulating phase and $g = 1/3$ for the metallic phase. The conductivity of superconducting spheres in a normal conductor is of the type $A_i = \infty$ and yields percolation at $f = 1/3$. More generally, the switching between inverse quantities, such as resistivity ρ and conductivity $\sigma = 1/\rho$, is realized by the transformation $g \rightarrow 1 - g$ in Eqs. (2) and (4). The mean-field character of Bruggeman percolation means that fluctuations are treated in a very crude way, on the level of Ornstein-Zernike correlation functions with the critical exponent $\nu = 1/2$ [23, 31]. This leads to inaccuracies in the predictions for A_{eff} near the percolation threshold.

The applicability of the Bruggeman theory to stationary transport processes, such as electrical conduction, thermal conduction, and diffusion, may be shown in two alternative ways. The first derivation exploits that conductivity and diffusion (A) involve generalized forces $\nabla \Phi$ that have the character of concentration, potential, or temperature gradients. The flux density \mathbf{j} is conserved, $\nabla \cdot \mathbf{j} = 0$, and obeys Fick's law, for example $\mathbf{j} = -D \nabla c$ for

diffusion. This yields Eq. (3) in the form $\nabla \cdot (D(\mathbf{r})\nabla c) = 0$ and leads to $g = N$. A second derivation is based on Maxwell's equation $\nabla \times \mathbf{H} = \mathbf{j} + \partial \mathbf{D} / \partial t$, which shows that the time derivative of the displacement is a current density, in analogy to the current necessary to charge a capacitor. Application of $\mathbf{E}(t) = \mathbf{E}_0 \exp(i\omega t)$ in combination with $\mathbf{D} = \epsilon \mathbf{E}$ and $\mathbf{j} = \sigma \mathbf{E}$ yields the complex permittivity $\epsilon^* = \epsilon - i\sigma/\omega$. This makes it possible to treat static and stationary phenomena on a common footing, by considering complex quantities such as $\epsilon'' = \epsilon' + i\epsilon''$.

A somewhat less well-known approach is the use of the Bruggeman theory for mechanical composites. There is a rich literature on small volume fractions [2, 32, 33], and true Bruggeman equations have later been obtained for various elastic, viscous, and viscoelastic materials [20]. It is instructive to extract generalized shape constants g for mechanical composites. For *spherical* inclusions, the shear modulus G and the bulk modulus K are described by

$$g = \frac{2(4 - 5\nu_0)}{15(1 - \nu_0)} \quad (5a) \quad \text{and} \quad g = \frac{1 + \nu_0}{3(1 - \nu_0)} \quad (5b)$$

respectively. In both equations, ν_0 is Poisson's ratio of the matrix. Taking typical solids with $\nu_0 \approx 0.35$ yields $g = 0.46$ for G and $g = 0.69$ for K . Incompressible materials (rubbers) have $\nu_0 = 1/2$, that is, $g = 2/5$ for G and $g = 1$ for K .

The shear stress in a viscoelastic material contains an elastic component $\sigma = G \epsilon$ and a viscous component $\sigma = \eta d\epsilon/dt$, and the complex shear modulus $G^* = G + i\omega\eta$ [2, 27]. When the material is incompressible, then both the viscosity and shear modulus exhibit $g = 2/5$. The corresponding Maxwell-Garnett relation, $\eta = \eta_0(1 + 2.5f)$, was first derived by Einstein [2, 32, 33], but $g = 2/5$ is easily derived by putting $\nu_0 \approx 1/2$ in Eq. 5(a). Incompressibility is realized in ordinary liquids, which are largely incompressible by nature, and in elastic (and viscoelastic) rubbers, where $K \gg G$ and $\nu_0 \approx 1/2$ [11]. In a very good approximation, this limit is realized for carbon-reinforced rubber composites, as used in car tires [11, 34]. Since $g = 2/5$, percolation is predicted when the volume fraction of rigid spheres reaches 40%. This is close to the experimental value of about 49% [2].

NONLINEAR AND LOCAL ENERGY AND ENTROPY EFFECTS

A counterintuitive feature of many composites is that an improvement of materials constants may actually lead to a *deterioration* of figures of merit. The first example comes from permanent magnetism, where an increased fraction of rare-earth atoms may be used to improve the coercivity (magnetic hardness) H_c of the material but deteriorates the energy product by reducing the magnetization. In more detail, H_c scales as $2K_1/M_s$ and can be made arbitrarily large by choosing materials with a small M_s . However, the energy product of a permanent magnet does not exceed $M_s^2/4$, so that this coercivity increase is not an option. The second example is metallic inclusions in dielectrics, which enhance the permittivity but tend to reduce the breakdown field and the electrostatic-energy density in a capacitor made from the composite material [17, 21, 35, 36, 37]. Elastic moduli are important for construction materials, but very often the main considerations are mechanical toughness and fracture behavior [38].

This deterioration of figures of merit of composites violates effective-medium theory, which predicts materials constant A_{eff} intermediate between A_m and A_i . There are two reasons for this effect, namely nonlinear and local mechanisms. First, the underlying materials equations are nonlinear, characterized by field-dependent materials constants. Even in materials with linear equations of state, figures of merits often have the character of energy densities rather materials constants, which introduces nonlinearity. Compared to the determination of effective materials constants, whose physics largely reduces to the determination of a single parameter (g), the nonlinearity yields an essential differentiation between different systems, not only between different classes of materials but also between different figures of merit for a single class of materials. The reason is that there are usually many ways of constructing energy functions from materials constants. For example, losses in soft-magnetic materials are described by the area of the M - H hysteresis loop, whereas the energy product of permanent magnets is equal to the largest rectangle fitting under the B - H loop in the 2nd quadrant of the magnetization curve, where $B = M + H$ [22]. In dielectric materials, the electrostatic energy $W = \int \eta \, dV$, where η is the electrostatic energy density. In the linear regime, $\eta = \int \mathbf{E} \, d\mathbf{D}$ yields $\eta = \frac{1}{2} \epsilon_0 \epsilon_r E_{\text{max}}^2$, but D is in general a nonlinear function of the field, which affects η [26, 33, 39]. In practice, the saturation polarization puts an upper limit to η , and E is limited by the breakdown field. For example, an external electric field may rotate or align nearly free dipoles, but the energy stored by this mechanism is very low.

Second, the Bruggeman theory is a mean-field approach, considering inclusions in an average environment and unable to account for long-range *fluctuations*. For example, electric breakdown may be realized via a percolating backbone, where the creation of a single percolation bond initiates the collapse of the electric field. The Bruggeman theory is poorly equipped to handle this scenario and yields, for example, incorrect critical exponents. Fluctuations often determine the main figures of merit of materials. For example, mechanical fracture tends to start at cracks [14], the dielectric storage capacity is limited by the maximum local electric field [35] (as contrasted to the average field), and the coercivity of permanent magnets is determined by the local rather than average anisotropy [9, 22]. In fact, the dielectric contrast caused by the embedding of a single high- ϵ particle in a low- ϵ matrix is known to shift field strength and energy density from the particles into the matrix and to substantially reduce the breakdown field. The effect depends on geometrical factors such as surface curvature of the particle surface [35].

Materials-specific breakdown, fracture, and coercivity mechanisms often yield a *logarithmic* dependence of materials constants and figures of merit on the system size L . Figures of merit describing the failure of dielectric and mechanical materials are often a power of $1/\ln(L)$, and a similar size dependence is encountered in permanent magnets [14, 22]. In the former case, the cracks responsible for mechanical failure may be modeled as ellipsoidal inclusions, which assimilates the mechanical problem to the dielectric problem [14]. The latter case may be understood by considering defect-containing models hard-magnetic particles in bonded or sintered magnets [22].

NANOSCALE EFFECTS

Breakdown phenomena are often realized on a nanoscale or even atomic scale [14], as epitomized by the mean free path of the electrons that realize the breakdown (scattering or capturing of electrons). A different question is the effective *interaction*

length $1/\kappa$ in dielectrics. Aside from affecting the break-down field, interactions may also yield a direct modification of materials constants if the inclusion size become comparable to the interaction range. The Bruggeman theory is unable to distinguish between macroscopic and nanoscale effects, because the partial differential equation $\nabla^2\Phi = 0$ does not involve a characteristic length. Nanoscale effects would require

$$\nabla^2\Phi - \kappa\Phi = 0 \quad (6)$$

where $1/\kappa$ can be interpreted as a screening length [4, 25, 40]. This screening length reflect the competition between different local and non-local energy contributions and is sometimes of the order of a few nanometers. It has far-reaching consequences for the understanding of advanced mechanical and electromagnetic composites, because the inclusion size tends to interfere with the length scale of the interaction.

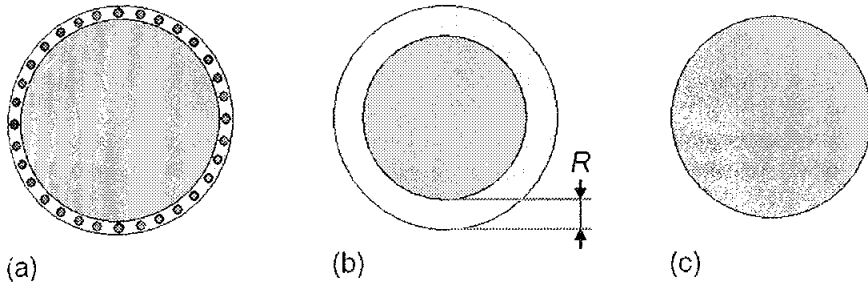


Fig. 2. Range of interaction effects: (a) atomic, (b) nanoscale, and (c) macroscopic.

Magnetic Composites

The magnetic permeability of some soft-magnetic composites is described by Eq. (4), but in general the finite saturation magnetization puts a limit to the applicability of the Bruggeman theory. Hard-soft nanocomposites magnets for permanent-magnet applications, which have been investigated quite intensively [4, 9, 22, 41], exhibit nontrivial nanoscale interactions. In these materials, the energy product is determined by the coercivity, which is, in a crude nucleation-field approximation [4, 9], obtained as the lowest-lying H eigenvalue of

$$-A\nabla^2m + (K_1(\mathbf{r}) - \frac{1}{2}\mu_0M_sH)m = 0 \quad (7)$$

Here A is the exchange stiffness and K_1 is the first uniaxial anisotropy constant. Equation (7) has the structure of Eq. (6), and both coercivity and energy product depend on the size of the hard and soft regions, as described by the local anisotropy $K_1(\mathbf{r})$. The corresponding interaction length is

$$\frac{1}{\kappa} = \sqrt{\frac{A}{K_1(\mathbf{r}) - \frac{1}{2}\mu_0M_sH}} \quad (8)$$

This means that g is a function of the radius of the hard inclusions rather than a constant. Physically, the hard-magnetic spheres create an 'interaction cloud' of a exchange-coupled soft-magnetic material.

The length $1/\kappa$ is essentially equal to the domain-wall width of the hard phase. In practice, it reaches several nanometers, in spite of the atomic origin of the two parameters A and $K_1(\mathbf{r})$. The reason is the relativistic smallness of K_1 [9, 42], meaning that $1/\kappa$ describes a competition between Heisenberg exchange, which is characterized by Curie temperatures of several 100 K, and magnetocrystalline anisotropy, which corresponds to energy equivalents of 1 K or less [23]. Consequently, magnetic domain walls are quite broad, from about 20 interatomic distances (5 nm) for very hard materials to more than 1000 interatomic distances in soft magnets. This length scale also determines the spin structure in nanospirals, Fig. 1(f). Note that the ferromagnetic (and ferroelectric) domain-wall width must not be confused with the actual domain size, which may be much larger.

The nanoscale range of the coupling is limited to the coercivity. Equations such as (7) cannot be used, for example, to determine effective Curie temperatures T_c . As analyzed elsewhere [23, 43], Curie temperatures differing by more than a few K mean that the phase with the lower T_c slightly polarizes the phase with the higher T_c , but the corresponding decay length is only a few interatomic distances. In a strict sense, the residual coupling is a thermodynamically equivalent to a ferromagnetic phase transition with a relatively high T_c , but for any practical purposes the Curie-temperature behavior is two-phase like.

Mechanical Composites

There is a wide range of mechanical composites, but our focus is on a specific case, namely reinforced rubbers, as used for car tires. The reinforcement is caused by small silica or carbon-black particles, and it is well-known that the use of nanoparticles drastically improves mechanical properties such as modulus and toughness. For 'ideal' or 'phantom' polymer networks, the shear modulus is $G_0 \approx nk_B T$, where n is the cross-link density, and Young's modulus is three times as large. For large particles, one can use the Einstein formula, $G = G_0 (1 + 2.5 f)$, which corresponds to Eq. (5) with $g = 2/5$.

High-performance fillers have particle radii of about 10 nm, which is comparable to the average end-to-end distance $R_N \sim N^{1/2}$ of the polymer chains [11, 34]. In other words, the average cross-link distance, which determines n and G , becomes comparable to the radius of the carbon or silica nanoparticles and leads to a complicated chain behavior in filled rubber [44, 45]. Figure 3 illustrates some of these chain configurations. Since the surface of the particle creates additional crosslinks, there is an additional 'Bueche' contribution proportional to the number of chains that touch a particle, which enhances G [34] and means that g becomes a function of R_N/R . However, $G_0 \approx nk_B T$ derives from the entropy reduction of the chains as the end-to-end distance increases under strain. Some chains, such as C in Fig. 3(a), do not exhibit a change in the end-to-end distance, so that their zeroth-order contribution to G_0 vanishes. This effect is also governed by the ratio R_N/R but qualitatively different from an enhanced cross-link density.

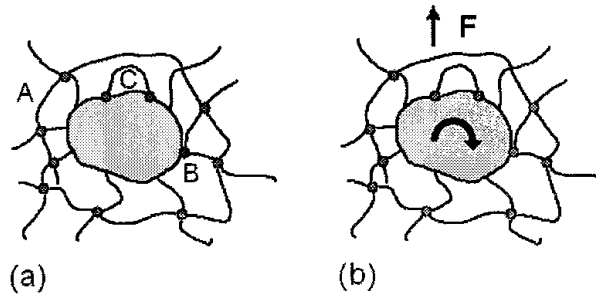


Fig. 3. Rubber reinforcement due to nanoparticles: (a) types of chains (A: phantom chain, B: extra crosslink, C: dead chain) and (b) behavior of the chain under strain. The toughness enhancement probably reflects the release of excessive strain due to particle motion and rotation (b).

Dielectric Composites

A key materials constant for dielectrics is the permittivity ϵ , as it appears in the electric energy density $w = \frac{1}{2} \epsilon E^2$. Since composites have materials constants intermediate between the materials constants of the individual phases, it is tempting to use composites where ϵ is enhanced by embedding inclusions that have a high ϵ , such as TiO_2 [25, 46]. In fact, metallic [35, 36] particles have an infinite permittivity and are ideally suited for ϵ -enhancement. The dielectric constant can be enhanced by embedding highly permittive particles in a matrix or using structures such as metallic grains separated by non-metallic grain boundaries [37]. In former years, it was difficult to create nanoparticles of very small sizes, which has led to problems such as eddy currents in metallic inclusions, but a recent development is that nanoparticles can now be produced on length scales of 5 nm or less [47], as compared to the submicron particles used in earlier research. However, as discussed above, the positive effect on ϵ is typically overcompensated by the reduction in break-down field.

An interesting question is how nanoscale phenomena affect dielectric composites and whether nanostructuring can be used improve the dielectric energy density. Gradient expressions similar to the exchange-stiffness term of Eq. (7) can be added to a Landau-type potential energies for dielectric polymers, but the question is the range of the exchange interaction. An exchange length of a few nanometers has recently been used to discuss core-shell particles in a polymeric matrix [25, 48], but the interaction range $1/\kappa$ is treated as an adjustable phenomenological parameter. Mindlin [49] considered the polarization gradient in the stored energy function of elastic dielectrics, but the interaction range is usually rather small, only a few Å in typical dielectric materials. In fact, Askar *et al.* [50] used a long-wavelength approximation to calculate an interaction length of about $1/\kappa \sim 0.2$ nm for some ionic compounds, without indication that other materials might exhibit robust interactions on a much larger length scale.

In magnetism, the exchange length reflects the relativistic competition between anisotropy energy E_a per atom and the Heisenberg exchange J , and this leads to a physically well-based hierarchy in terms of Sommerfeld's fine structure constant, $E_a/J \sim (1/137)^2$ [42]. In dielectric materials, there is no comparable hierarchy. The interface acts

as a perturbation and locally changes the polarization of the adjacent phases, but the extra polarization costs energy and decreases quite rapidly with increasing distance from the interface. In fact, cohesive and dielectric energies are of comparable orders of magnitude, as epitomized by typical ferroelectric Curie and melting temperatures, respectively.

Figure 4 illustrates how nanoscale interactions may be realized in dielectrics. The model assumes dipoles separated by a segment length a and having a polarization $P_i(x) = P_0 \cos(\theta_i)$, subjected to an electric field that points in the z direction. The dipoles can freely rotate in the y - z plane, but there is a coupling $-K \cos(\theta_i - \theta_j)$ between neighboring dipoles. The free chain (a) gets easily polarized by the electric field (high ϵ but low energy density $w \sim 1/\epsilon$), whereas the coupled chain (b) can store a relatively large energy associated with the torque interaction constant K . The permittivity and energy density depend on the interaction length $L \sim a \sqrt{K/P_0 E}$ and on the particle spacing, and by adjusting the latter, one can optimize the performance of the structure.

In a few cases, electric interactions may be long range, with a $1/r^m$ power-law distance dependence of the interaction strength. One example is the switching of the magnetization in insulating multiferroic composites that contain dielectric and rare-earth magnet regions [23, 51]. Here the electric dipoles create a crystal-field contribution that scales as $1/r^4$ and interacts with the electric quadrupole moment of the tripositive rare-earth ions. Due to the rigid spin-orbit coupling of the rare earths, this can be used to switch the magnetization direction.

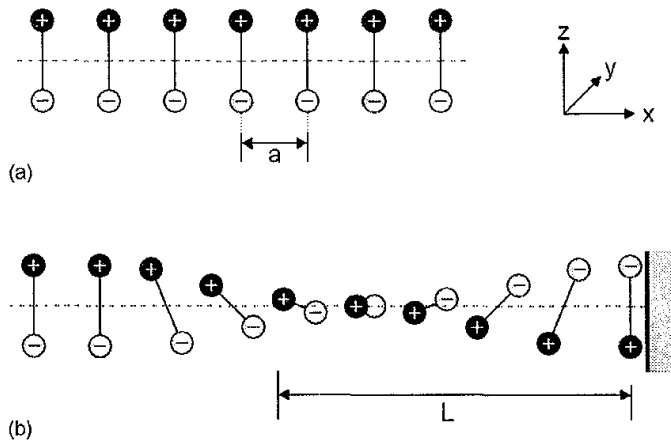


Fig. 4. Nanoscale interaction effects in a dielectric polymer model: (a) free chain and (b) chain adsorbed to a nanoparticle (right).

DISCUSSION AND CONCLUSIONS

In summary, we have investigated how different magnetic, mechanical and dielectric properties are affected by nanostructuring. Length-scale independent effective-field theories, whose physics is contained in a single shape parameter g , yield reasonable volume-averaged materials parameters and even provide a qualitative description of

percolation phenomena. However, physical figures of merit tend to have the character of energy densities, which introduces a considerable complexity and diversity in the description of composite materials. Examples are the dependence of the dielectric energy on the permittivity of the oxide or metal inclusions and the energy-product enhancement in magnetic two-phase nanocomposites. A further complication is due to nanoscale phenomena, which affects coercivity, break-down, and fracture, and often lead to a logarithmic dependence of figures of merit on the macroscopic size of the considered body. Nanoscale interaction lengths are materials- and property-specific, as contrasted to the length-scale independent character of effective-field theories.

ACKNOWLEDGEMENT

This work is supported by NSF-MRSEC, ONR, and NCMN. The authors are grateful to S. Ducharme and K. Kraemer for discussing various aspects of dielectric composites.

REFERENCES

- [1] D. A. G. Bruggeman, *Ann. Phys.* (5) **24** (1935) 637.
- [2] R. M. Christensen, *Mechanics of Composite Materials*, Wiley, New York 1979.
- [3] C. Verdier, *J. Theor. Med.* **5** (2003) 67.
- [4] R. Skomski, *J. Phys.: Condens. Matter* **15** (2003) R841.
- [5] A. Chipara, D. Hul, J. Sankar, D. Leslie-Pelecky, A. Bender, L. Yue, R. Skomski, and D. J. Sellmyer, *Composites B: Engineering* **35** (2004) 235.
- [6] M. Chipara, R. Skomski, D. J. Sellmyer, *Mater. Lett.* **61** (2007) 2412.
- [7] N. Ali, M. Chipara, S. Balascuta, R. Skomski, and D. J. Sellmyer, *J. Nanosci. Nanotechnol.* **9** (2009) 4437.
- [8] J. C. M. Garnett, *Philos. Trans. R. Soc. (London) A* **203** (1904) 385.
- [9] R. Skomski and J. M. D. Coey, *Phys. Rev. B* **48** (1993) 15812.
- [10] Z. Hashin and S. Shtrikman, *J. Appl. Phys.* **33** (1962) 3125.
- [11] B. Erman and J. E. Mark, *Structures and Properties of Rubberlike Networks*, Oxford University Press, Oxford 1997.
- [12] J. M. Dewey, *J. Appl. Phys.* **18** (1947) 578.
- [13] D. Schmidt, A. C. Kjerstad, T. Hofmann, R. Skomski, E. Schubert, and M. Schubert, *J. Appl. Phys.* **105** (2009) 113508.
- [14] B. K. Chakrabarti and L. G. Benguigui, *Statistical Physics of Fracture and Breakdown in Disordered Systems*, University Press, Oxford 1997.
- [15] R. Skomski, J.-Y. Li, J. Zhou, and D. J. Sellmyer, in: *Materials for Space Applications*, Eds. M. Chipara, D. L. Edwards, R. S. Benson, S. Phillips, *Mater. Res. Soc. Symp. Proc.* **851** (2005) NN1.7.
- [16] D. Polder and J. H. van Santen, *Physica* **12** (1946) 257.
- [17] K. K. Kärkkäinen, A. H. Sihvola, and K. I. Nikoskinen, *IEEE Trans. Geosci. and Remote Sensing* **38** (2000) 1303.
- [18] B. Velický, S. Kirkpatrick, and H. Ehrenreich, *Phys. Rev.* **175** (1968) 747.
- [19] S. Kirkpatrick, *Phys. Rev. Lett.* **27** (1971) 1722.
- [20] T. C. Choy, *Effective Medium Theory*, University Press, Oxford 1999.

- [21] W. T. Doyle, *J. Appl. Phys.* **85** (1999) 2323.
- [22] R. Skomski and J. M. D. Coey, *Permanent Magnetism*, Institute of Physics, Bristol 1999.
- [23] R. Skomski, *Simple Models of Magnetism*, University Press, Oxford (2008).
- [24] Z. Hashin, *J. Appl. Mech.* **29** (1962) 143.
- [25] J. Y. Li, L. Zhang, and S. Ducharme, *Appl. Phys. Lett.* **90** (2007) 132901.
- [26] O. Levy and D. Stroud, *Phys. Rev. B* **56** (1997) 8035.
- [27] I. M. Ward and D. W. Hadley, *Mechanical Properties of Solid Polymers*, Wiley, New York 1993.
- [28] P. Banerjee, I. Perez, L. Henn-Lecordier, S. B. Lee, and G. W. Rubloff, *Nature Nanotechnology* **4** (2009) 292.
- [29] A. Lakhtakia, B. Michel, and W. S. Weiglhofer, *J. Phys. D: Appl. Phys.* **30** (1997) 230.
- [30] J. A. Osborn, *Phys. Rev.* **67** (1945) 351.
- [31] J. M. Yeomans, *Statistical Mechanics of Phase Transitions*, University Press, Oxford 1992.
- [32] T. S. Chow, *Mesoscopic Physics of Complex Materials*, Springer, Berlin 2000.
- [33] A. Einstein, *Ann. Phys.* **19**, 289 (1906); Erratum: **34** (1911) 591.
- [34] R. Skomski, *Theory of Elasticity of Filled Polymer Networks*, THLM Leuna-Merseburg (Diplomarbeit, unpublished, 1986).
- [35] P. M. Duxbury, P. D. Beale, H. Bak and P. A. Schroedert, *J. Phys. D:* **23** (1990) 1546.
- [36] Zh.-M. Dang, Y.-H. Lin, and C.-W. Nan, *Adv. Mater.* **15** (2003) 1625.
- [37] J.-H. Kim, Y.-W. Lee, M. G. Kim, A. Souchkov, J. S. Lee, H. D. Drew, S.-J. Oh, C. W. Nan, and E. J. Choi, *Phys. Rev. B* **70** (2004) 172106.
- [38] G. Murphy, *Advanced Mechanics of Materials*, McGraw-Hill, New York 1946.
- [39] H. E. Alper and R. M. Levy, *J. Phys. Chem.* **94** (1990) 8401.
- [40] R. Skomski, *J. Magn. Magn. Mater.* **272-276** (2004) 1476.
- [41] R. Coehoorn, D.B. de Mooij, and C. de Waard, *J. Magn. Magn. Mater.* **80** (1989) 101.
- [42] R. Skomski, H.-P. Oepen, and J. Kirschner, *Phys. Rev. B* **58** (1998) 3223.
- [43] R. Skomski and D. J. Sellmyer, *J. Appl. Phys.* **87** (2000) 4756.
- [44] A. Botti, W. Pyckhout-Hintzena, D. Richter, V. Urban, and E. Straube *J. Chem. Phys.* **124**, 174908 (2006).
- [45] E. Straube, V. Urban, W. Pyckhout-Hintzen, D. Richter, and C. J. Glinka, *Phys. Rev. Lett.* **74**, 4464 (1995).
- [46] G. F. Dionne, J. F. Fitzgerald, and R. C. Aucoin, *J. Appl. Phys.* (1976) 1708.
- [47] B. Balamurugan, K. L. Kraemer, N. A. Reding, R. Skomski, S. Ducharme, and D. J. Sellmyer, *ACS Nano* **4** (2010) 1893.
- [48] J. Y. Li, *Phys. Rev. Lett.* **90** (2003) 217601.
- [49] R. D. Mindlin, *International Journal of Solids and Structures* **4** (1968) 637.
- [50] A. Askar, P. C. Lee, and A. S. Cakmak, *Phys. Rev. B* **1-3537** (1970) 3525.
- [51] R. Skomski, A. Kashyap, and A. Enders, *J. Appl. Phys.*, in press (2011).